© 2022. Published by The Company of Biologists Ltd | Journal of Cell Science (2022) 135, jcs259272. doi:10.1242/jcs.259272

RESEARCH ARTICLE

MCC is a centrosomal protein that relocalizes to non-centrosomal apical sites during intestinal cell differentiation

Lucian B. Tomaz[1,2,3], Bernard A. Liu[4], Meroshini M[1], Sheena L. M. Ong[3], Ee Kim Tan[1,3], Nicholas S. Tolwinski[5], Christopher S. Williams[6], Anne-Claude Gingras[4,7], Marc Leushacke[8] and N. Ray Dunn[1,2,3,8,*]

ABSTRACT

The gene mutated in colorectal cancer (*MCC*) encodes a coiled-coil protein implicated, as its name suggests, in the pathogenesis of hereditary human colon cancer. To date, however, the contributions of MCC to intestinal homeostasis and disease remain unclear. Here, we examine the subcellular localization of MCC, both at the mRNA and protein levels, in the adult intestinal epithelium. Our findings reveal that *Mcc* transcripts are restricted to proliferating crypt cells, including *Lgr5*+ stem cells, where the Mcc protein is distinctly associated with the centrosome. Upon intestinal cellular differentiation, Mcc is redeployed to the apical domain of polarized villus cells where non-centrosomal microtubule organizing centers (ncMTOCs) are positioned. Using intestinal organoids, we show that the shuttling of the Mcc protein depends on phosphorylation by casein kinases 1δ and ε, which are critical modulators of WNT signaling. Together, our findings support a role for MCC in establishing and maintaining the cellular architecture of the intestinal epithelium as a component of both the centrosome and ncMTOC.

KEY WORDS: MCC, Centrosome, ncMTOCs, Protein relocalization, Phosphorylation, Intestine

INTRODUCTION

The gene mutated in colorectal cancer (*MCC*) was identified through cytogenetic and linkage studies in 1991 as a culprit tumor suppressor gene for the autosomal dominant human hereditary colon cancer syndrome familial adenomatous polyposis (FAP) (Ashton-Rickardt et al., 1991; Kinzler et al., 1991b). FAP patients typically present with hundreds to thousands of adenomas in the colon and rectum (Waller et al., 2016). Later the same year, the gene adenomatous polyposis coli (*APC*), which is tightly linked to *MCC* on human chromosome 5q21, was correctly established as the gene responsible for FAP (Groden et al., 1991; Kinzler et al., 1991a; Nishisho et al., 1991). Despite its historical association with colorectal cancer (CRC), linkage to *APC* and strong evolutionary conservation (Luongo et al., 1993), *MCC* transcript distribution, the subcellular localization of the MCC protein and its precise function in the intestine have not been fully characterized.

The *MCC* gene encodes a large coiled-coil protein harboring a highly conserved, extreme C-terminal type I PSD-95–Dlg–ZO-1 (PDZ)-binding motif (PBM) (Bourne, 1991; Arnaud et al., 2009; Pangon et al., 2012). Depending on the cell line, tissue, reagent or assay used, MCC has been found in several organelles (mitochondria and endoplasmic reticulum) and cellular compartments (plasma membrane, cytoplasm and nucleus) (Arnaud et al., 2009; Benthani et al., 2018; Fukuyama et al., 2008; Senda et al., 1997; Matsumine et al., 1996; Pangon et al., 2010). These discrepant results have cast doubt about the precise role that MCC serves within a cell. For example, MCC is known to be a phosphoprotein, with phosphorylation of amino acid 827 at position −1 within the C-terminal PBM required for its interaction with the PDZ-domain containing protein scribble (SCRIB) at the active migratory edge of CRC cell lines (Pangon et al., 2012; Caria et al., 2019). When overexpressed, MCC has been shown to bind β-catenin (CTNNB1) in the nucleus to negatively regulate canonical WNT signaling in cancer cell lines and to inhibit cell proliferation (Fukuyama et al., 2008; Pangon et al., 2015). In contrast, a recent report argues that MCC is membrane associated and interacts with β-catenin and E-cadherin to strengthen cell adhesion in CRC cell lines (Benthani et al., 2018). These confounding results motivated us to identify the MCC protein interactome in an effort to firmly define its subcellular localization and function.

Here, we show for the first time that MCC associates with the protein interaction network that surrounds the centrosome in assorted cell lines and within mouse and human proliferating intestinal crypt cells. The centrosome is the main microtubule-organizing center (MTOC) in most proliferative cells (Brinkley, 1985; Muroyama and Lechler, 2017). However, centrosomes are often inactivated or severely attenuated upon cell cycle exit and terminal differentiation, with MTOC function being reassigned to diverse and cell-specific sites termed non-centrosomal microtubule-organizing centers (ncMTOCs) (Meads and Schroer, 1995; Goldspink et al., 2017b; Muroyama and Lechler, 2017). Little is known about the composition and regulatory mechanisms underlying the formation of ncMTOCs. During intestinal epithelial cell differentiation, we find that the murine Mcc protein redeploys from the MTOC in crypt cells to the apical domain of villus differentiated cells, incorporating into the ncMTOC. Finally, we provide evidence that the relocalization of the Mcc protein from the MTOC to the apical ncMTOC is governed by casein kinase 1δ (CK1δ) and ε (CK1ε) phosphorylation, whose interaction with MCC was revealed by our proteomics studies and implicates WNT signaling in the crucial events that sustain intestinal homeostasis.

[1]Lee Kong Chian School of Medicine, Nanyang Technological University, 308232, Singapore. [2]School of Biological Sciences, Nanyang Technological University, 637551, Singapore. [3]Institute of Medical Biology, Agency for Science, Technology and Research (A*STAR), 138648, Singapore. [4]Lunenfeld Tanenbaum Research Institute, Mount Sinai Hospital, Sinai Health, Toronto, ON M5G 1X5, Canada. [5]Division of Science, Yale-NUS College, 138527, Singapore. [6]Department of Medicine, Vanderbilt University Medical Center, Nashville, TN 37232, USA. [7]Department of Molecular Genetics, University of Toronto, Toronto, ON M5S 1A8, Canada. [8]Skin Research Institute of Singapore, Agency for Science, Technology and Research (A*STAR), 308232, Singapore.

*Author for correspondence (ray.dunn@ntu.edu.sg)

S.L.M.O., 0000-0002-7569-7944; N.S.T., 0000-0002-8507-2737; N.R.D., 0000-0002-6259-2975

Handling Editor: Jennifer Lippincott-Schwartz
Received 13 August 2021; Accepted 27 September 2022

Journal of Cell Science (2022) 135, jcs259272. doi:10.1242/jcs.259272

RESULTS

Mcc is specifically expressed in crypts of the intestinal epithelium

The intestinal epithelium is a constantly renewing single cell layer organized into crypt and villus units (Fig. 1A) (Gehart and Clevers, 2019). Finger-like villi harboring differentiated epithelial cells project into the intestinal lumen to facilitate nutrient absorption. Each villus is encircled by multiple contiguous, proliferative crypt compartments embedded within the underlying submucosa that contains crypt base columnar (CBC) stem cells (Leushacke and Barker, 2014; Barker, 2014; Clevers, 2013). We previously reported that *Mcc* is expressed in the adult mouse intestine using a

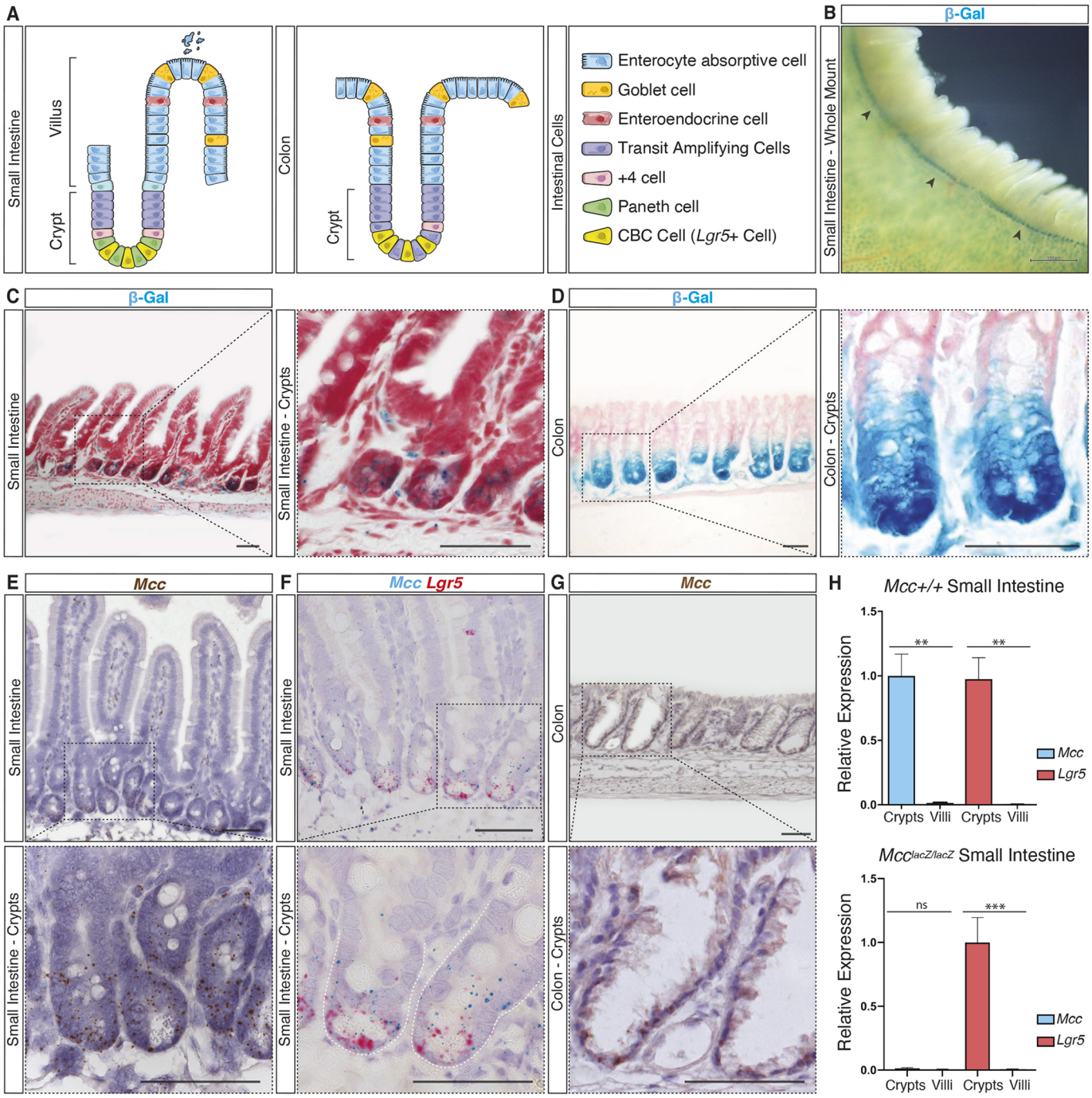

Fig. 1. *Mcc* is specifically expressed in crypts of the intestinal epithelium. (A) Schematic representation of small intestine (SI) and colon epithelial cellular organization. (B) Histochemical (HC) staining for β-galactosidase (β-Gal) activity in whole-mount $Mcc^{lacZ/lacZ}$ SI. Black arrowheads indicate β-gal activity (blue) restricted to crypt units. Scale bar: 500 µm. (C,D) HC for β-Gal activity on sections of $Mcc^{lacZ/lacZ}$ SI and colon tissues counter-stained with Nuclear Fast Red. Scale bars: 50 µm. (E–G) Section *in situ* hybridization (ISH) on wild-type (WT) SI and colon tissues. (E) Endogenous *Mcc* expression is specifically observed in crypts. (F) *Mcc* (blue) expression overlaps with *Lgr5* (red) at the crypt base but extends into the transit-amplifying compartment. (G) Endogenous *Mcc* expression on WT colonic crypts. Scale bars: 50 µm. Black-dashed squares in C–G highlight regions selected for higher magnification. All images shown are representative of at least five experiments. (H) qPCR analysis for *Mcc* and *Lgr5* in purified crypt and villus fractions from WT and homozygous Mcc^{lacZ} (*Mcc* null) mice. Results are mean±s.e.m., n=3. ***P<0.001; **P<0.01; ns, not significant (unpaired two-tailed t-test).

Journal of Cell Science (2022) 135, jcs259272. doi:10.1242/jcs.259272

Mcc^{lacZ} reporter allele generated by a gene-trap insertional mutation that results in premature termination of the *Mcc* transcript and, consequently, produces no Mcc protein (Young et al., 2011). However, the specific cell populations expressing *Mcc* in the crypt and villus were not fully characterized. We therefore re-examined *Mcc*^{lacZ} expression by detecting β-galactosidase (β-Gal) activity using carefully controlled 5-bromo-4-chloro-3-indolyl-β-d-galactopyranoside/ferri-/ferrocyanide (X-Gal) histochemistry (Merkwitz et al., 2016). We found that β-Gal activity is restricted to crypt units in both the small intestine (Fig. 1B,C) and colon (Fig. 1D). Co-staining for β-Gal and intestinal alkaline phosphatase (IAP) activity, a marker for differentiated villus cells (Sussman et al., 1989; Hinnebusch et al., 2004), in mechanically isolated crypt and villus fractions revealed that β-Gal-positive cells are distributed along the entire crypt, but not in the villus (Fig. S1A,B). Importantly, no detection of β-Gal activity was observed in whole-mount wild-type (WT) crypt fractions used as a negative control for our X-Gal histochemical analysis (Fig. S1B).

Next, we performed high-resolution RNA section *in situ* hybridization (ISH) for endogenous *Mcc* transcripts singly or in combination with leucine-rich repeat containing g-protein coupled receptor 5 (*Lgr5*), whose expression specifically labels CBC cells (Barker et al., 2007) (Fig. 1A,E–G; Fig. S1C,D). *Mcc* and *Lgr5* transcripts overlapped in CBC cells at the crypt base, whereas *Mcc* transcripts extended distally into the transit-amplifying (TA) compartment (Fig. 1A,E,F). Similarly, *Mcc* expression was restricted to crypts of the colonic epithelium (Fig. 1A,G). We further showed that *Mcc* and *Lgr5* were co-expressed in intestinal crypts using quantitative PCR (qPCR) (Fig. 1H). Taken together, our findings show that *Mcc* expression is entirely absent in differentiated cells of the small intestine (SI) and colon epithelia.

Proteomics analyses reveal MCC as a centrosomal protein

To provide insight into both MCC protein function and subcellular localization in the intestine, we first chose to establish the MCC protein–protein interactome in HEK293 cells, which express MCC endogenously (Arnaud et al., 2009). To accomplish this, we overexpressed FLAG-tagged human MCC followed by immunoprecipitation with anti-FLAG agarose beads and mass spectrometry (MS). Significance Analysis of INTeractome (SAINTexpress) of triplicate purifications of FLAG–MCC against triplicate analyses of negative controls (empty vectors) revealed 27 high-confidence MCC interactors, ten of which have been previously reported in the BioGRID interaction repository (Oughtred et al., 2021) (Table S2; Fig. S2A). The high-confidence MCC interactors significantly enriched Gene Ontology (GO) Molecular Function (MF) terms were cadherin binding (GO: 0045296, padj=2.835×10^{-6}) and cell adhesion molecule binding (GO: 0050839, padj=7.631×10^{-6}), and the Cellular Component (CC) terms were cytoskeleton (GO: 0005856, padj=2.006×10^{-8}) and centrosome (GO: 0005813, padj=1.256×10^{-4}).

Specifically, MCC interacts with several centrosomal proteins, such as CEP131, CEP170 and NDE1, with the casein kinases CSNK1D (CK1δ) and CSKN1E (CK1ε); and with PDZ-domain containing polarity proteins such as SCRIB, SNX27, DLG1, SNTB2 and NHERF2 (also known as SLC9A3R2) (Fig. 2A). Several proteins that regulate small GTPases were also recovered, including RASAL2, IQGAP1, GAPVD1 (GAPEX5) and RAB11FIP5 (RIP11) (Fig. 2A). Several of these interactions were independently confirmed by immunoprecipitation of Myc-tagged MCC and western blotting for endogenous proteins, including NDE1, CEP131 and CEP170, SCRIB and CK1ε (Fig. 2B). We further confirmed that the interaction between MCC and both SCRIB and the NHERF2 paralog NHERF1 (SLC9A3R1) (Arnaud et al., 2009; Pangon et al., 2012) was completely dependent on the extreme C-terminus PBM of MCC (Fig. S2B).

Several reports have described the subcellular localization of MCC, with often conflicting results (Arnaud et al., 2009; Benthani et al., 2018; Fukuyama et al., 2008; Senda et al., 1997; Matsumine et al., 1996; Pangon et al., 2010). Our interactome studies provided the first indication that MCC might reside at the centrosome. To explore this possibility, we generated an N-terminal *EmGFP-Mcc* expression construct and transfected it into HEK293 cells. We observed colocalization of GFP with endogenous pericentrin (PCNT), a component of the pericentriolar material (PCM) of the centrosomal complex (Doxsey et al., 1994) (Fig. 2C). To further characterize MCC localization, we identified a commercially available antibody that shows highly specific staining for endogenous MCC by immunofluorescence (IF) (Table S1). We then performed IF for MCC and PCNT as well as another well-characterized centrosomal protein, ninein (NIN) (Doxsey et al., 1994; Bouckson-Castaing et al., 1996) in a variety of cell lines, including RPE-1, SW480, HEK293 and HTC116 cells. Microscopy analysis using both confocal and super-resolution techniques such as structured illumination microscopy (SIM) (Heintzmann and Huser, 2017) confirmed MCC colocalization with either PCNT or NIN (Fig. 2D,E; Fig. S2D; Movie 1). We also detected colocalization of MCC at the centrosome with several of its interacting partners identified by MS, including CEP170, NDE1, CEP131 and NHERF1 (Fig. S2E). Quantitative analysis of numerous IF images in RPE-1 cells revealed that the colocalization of MCC with NINEIN, CEP170, NDE1, CEP131 and NHERF1 shows a strong positive correlation [Pearson correlation coefficient (r>0.5)] (Fig. S2F).

In summary, our study using a combination of MS, tagged protein overexpression and extensive IF reveals that MCC is a protein associated with the centrosome. We attribute the difference between our present results and earlier observations to technical factors involving the antigenicity of centrosomal proteins, including the choice of fixation and permeabilization reagents, as previously discussed, as well as antibody selection (Hua and Ferland, 2017; Goldspink et al., 2017a).

Mcc localizes to the centrosome in crypt cells and apical membrane of villus cells

We next performed IF for Mcc in mouse and human intestinal sections. Confocal microscopy confirmed that Mcc specifically localizes to the centrosome in proliferating crypt cells of both the SI (Fig. 3A,B; Fig. S3A,C) and colon (Fig. S4E). Strikingly, however, we observed highly specific staining for Mcc at the apical membrane of differentiated cells in the villus compartment (Fig. 3C,D; Fig. S3B,D) and at the surface of the colonic epithelium (Fig. S4E). No signal for Mcc was detected in crypt and villus sections of homozygous *Mcc*-null mice, which were used as a negative control for all IF analyses (Fig. S3C,D). We additionally examined the presence of Mcc protein in lysates from purified crypt and villus fractions by western blotting. Consistent with our IF results, Mcc protein was detected in WT crypt and villus fractions (Fig. 3E). Moreover, we observed colocalization of Mcc with Pcnt at the centrosome in crypt cells (Fig. 3F,H; Fig. S3F) and Mcc either with Pcnt or Ninein at the apical membrane in differentiated villus cells (Fig. 3F,G; Fig. S3F,G). Collectively, our findings show that Mcc specifically localizes to the centrosome (MTOC) in intestinal crypt cells and as cells undergo terminal

Journal of Cell Science (2022) 135, jcs259272. doi:10.1242/jcs.259272

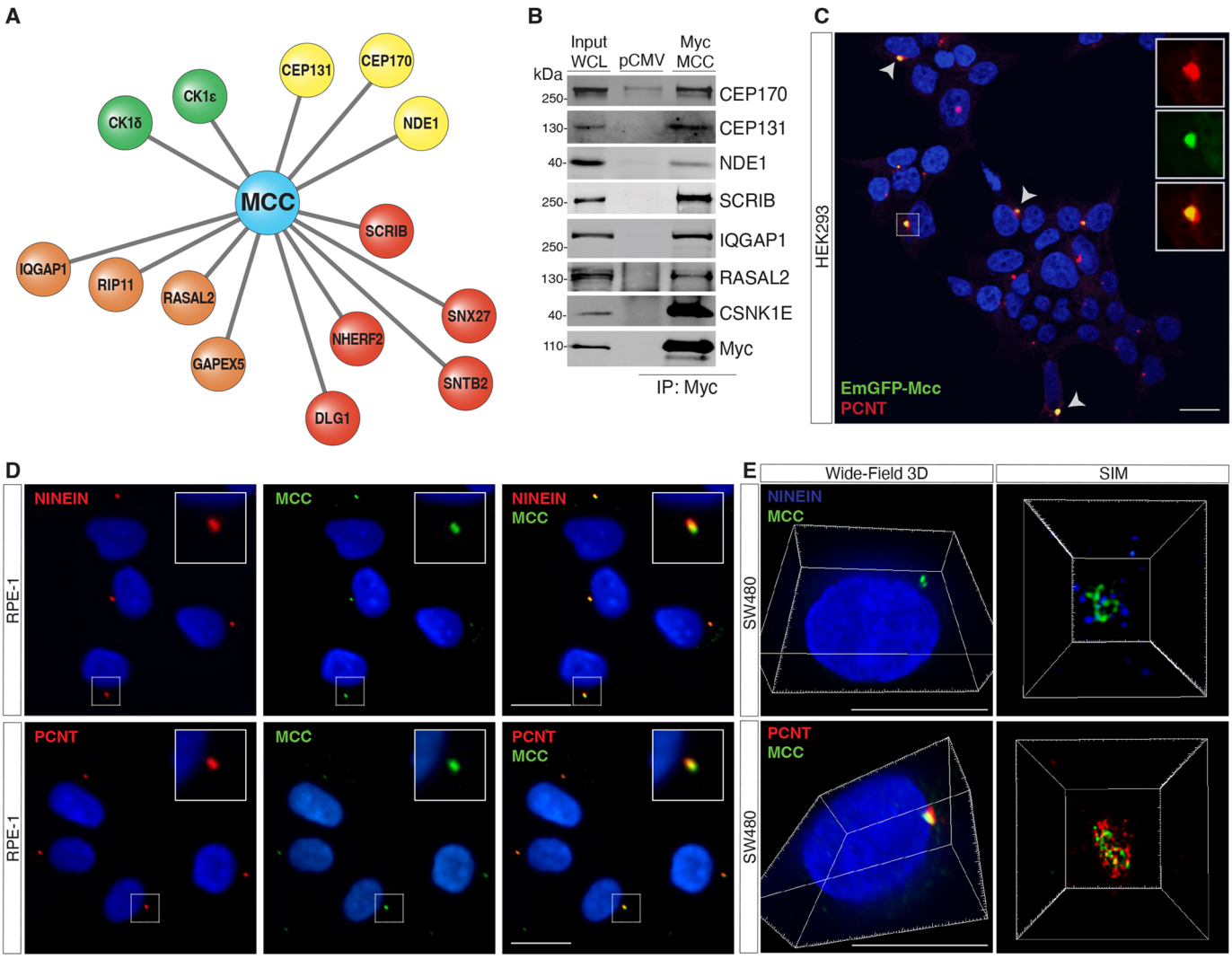

Fig. 2. Proteomics analyses reveal MCC interactome. (A) Immunoprecipitation (IP) of FLAG-tagged human MCC in HEK293 cells followed by mass spectrometry identifies various MCC interactors, including centrosomal proteins (yellow), PDZ-domain-containing polarity proteins (red), GTPase regulators (orange), and kinases (CSNK1E/D) (green). (B) IP of Myc-tagged human MCC in HEK293 cells followed by western blotting for the indicated interactions. WCL, whole-cell lysate; pCMV, pCMV empty vector control. (C) HEK293 cells transfected with EmGFP–Mcc. Arrowheads indicate colocalization of EmGFP–Mcc with the centrosomal protein pericentrin (PCNT). Insets show single channels for EmGFP–Mcc and PCNT immunostaining. Scale bar: 20 µm. (D) Immunofluorescence (IF) for MCC and ninein or PCNT shows colocalization at the centrosome in human RPE-1 cells. (E) IF 3D widefield showing MCC colocalizing with PCNT and NINEIN. Scale bars: 50 µm. Super-resolution structured illumination microscopy (SIM) shows spatial proximity between MCC and ninein or PCNT at the centrosome in SW480 cells. All images shown are representative of at least five experiments.

differentiation, Mcc is redeployed to the ncMTOC at the apical membrane of differentiated villus cells.

Phosphorylation by CK1δ and/or CK1ε triggers MCC redeployment to the ncMTOC at the apical membrane of villus cells

MCC is a phosphoprotein (Pangon et al., 2012; Caria et al., 2019; Arnaud et al., 2009). Importantly, among the MCC-interacting proteins uncovered by our MS analysis are two casein kinase 1 proteins (CK1δ and ε; hereafter collectively referred to as CK1δ/ε), which are known to play both positive and negative roles in the WNT/β-catenin signaling pathway and have regulatory functions at the centrosome (Peters et al., 1999; Sakanaka et al., 1999; Gao et al., 2002; Cruciat, 2014; Greer et al., 2014). We therefore asked whether MCC is a direct target of CK1δ/ε phosphorylation. Western blot analysis of SW480 cell lysates confirmed two closely migrating bands of endogenous MCC, one at 93 kDa, which is consistent with the predicted molecular mass of the unmodified protein (Pangon et al., 2010), and a second, higher molecular mass protein that was absent following treatment of the cells with PF670462 (Fig. 4A), a highly specific inhibitor of CK1δ/ε (Badura et al., 2007; Keenan et al., 2018). This result indicates that MCC is a target of CK1δ/ε phosphorylation. To confirm this finding, we co-expressed Myc–MCC with either FLAG–CK1ε or a catalytically inactive form of CK1ε (FLAG–CK1ε^{D128A}) in HEK293 cells. Only the active form of CK1ε induced an upward mobility shift of MCC (Fig. 4B). We additionally confirmed that overexpression of Myc–MCC and FLAG–CK1ε in the presence of PF670462 abolishes the higher molecular mass form of MCC, revealing that phosphorylation of MCC is triggered by CK1ε (Fig. 4C).

We predicted that phosphorylation of MCC by CK1δ/ε decreases its affinity for interacting partners at the centrosome, hence driving its relocalization to the apical ncMTOC in intestinal cells. To test this hypothesis, we overexpressed Myc–MCC singly or in

Journal of Cell Science (2022) 135, jcs259272. doi:10.1242/jcs.259272

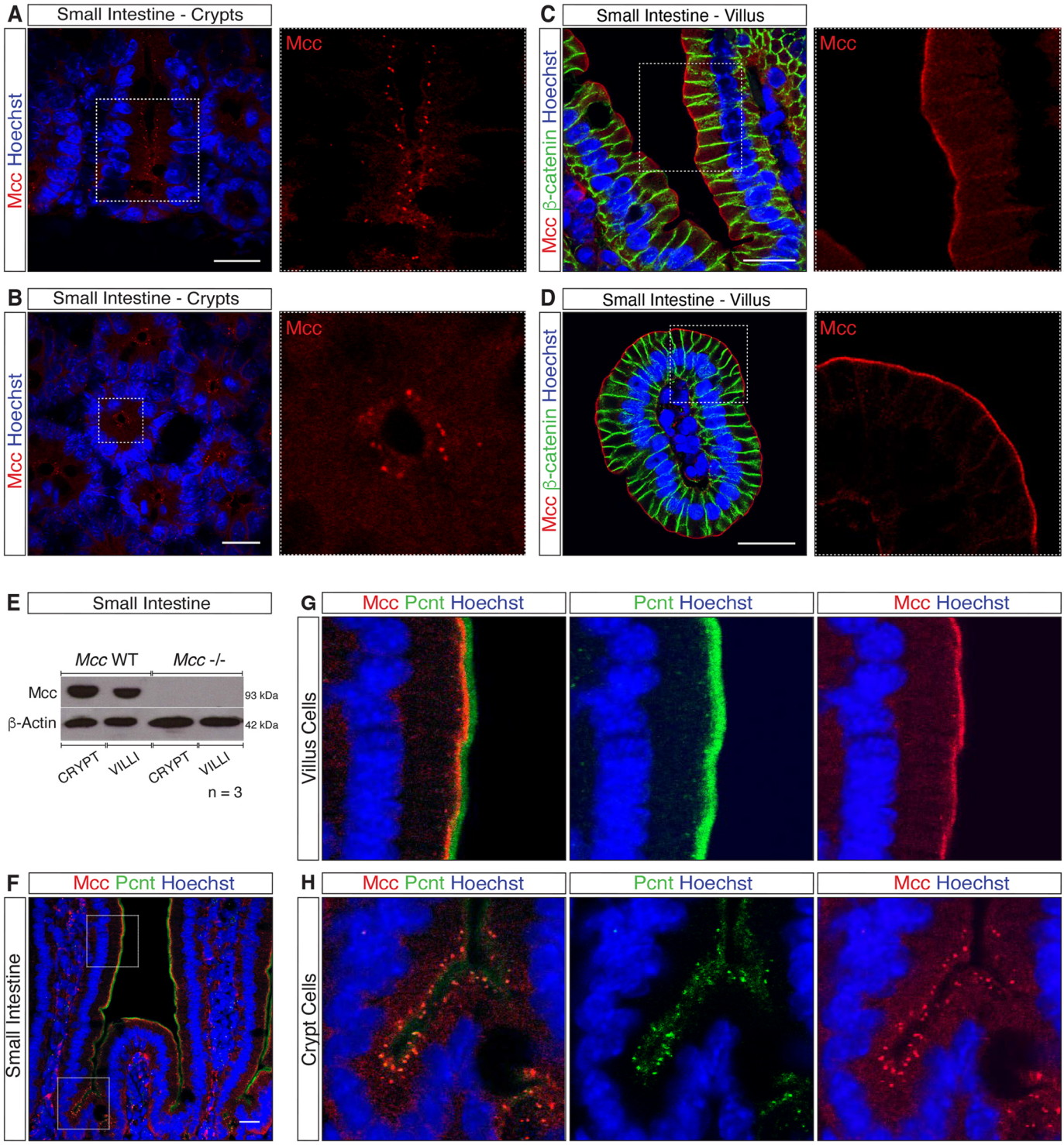

Fig. 3. Mcc localizes to the centrosome in crypt cells and apical membrane of villus cells. (A–D) Immunofluorescence (IF) for Mcc in the mouse small intestine (SI). White-dashed squares highlight regions selected for higher magnification (A and C, longitudinal and B and D, transverse sections). (A,B) Punctate centrosomal staining for Mcc is observed in crypt cells. (C,D) IF for Mcc and β-catenin in SI villi. Mcc localizes to the apical membrane whereas β-catenin labels the lateral membrane of villus cells. Scale bars: 20 µm. (E) Western blot for Mcc in whole-cell lysates from purified crypt and villus fractions of the mouse SI. (F) IF showing colocalization of Mcc with the centrosomal protein Pericentrin (Pcnt) in the crypt and villus units of the mouse SI. White-dashed squares highlight regions selected for higher magnification shown in G and H. Scale bars: 20 µm. All images shown are representative of at least five experiments.

combination with FLAG–CK1ε in HEK293 cells and immunoblotted for the centrosomal protein NDE1 along with the GTPase regulator protein RASAL2. We observed that in cells with CK1ε-induced MCC phosphorylation (+ Myc–MCC and+FLAG–CK1ε), the interaction with RASAL2 is stabilized, whereas binding to NDE1 is diminished, indicating that interactions between MCC and centrosomal proteins change upon phosphorylation (Fig. 4D; Fig. S2C).

Journal of Cell Science (2022) 135, jcs259272. doi:10.1242/jcs.259272

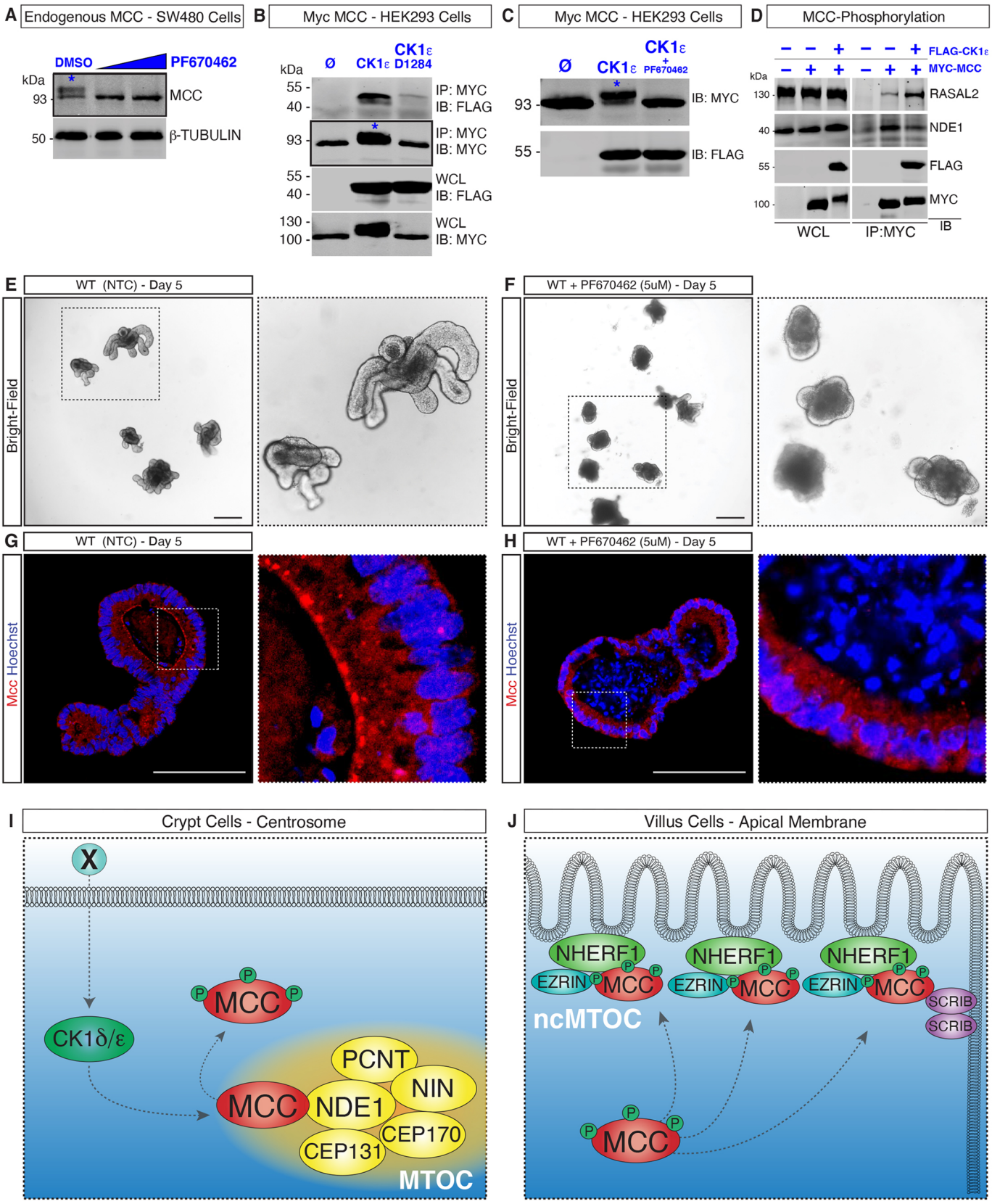

Fig. 4. See next page for legend.

We next generated *ex vivo* small intestinal organoids that faithfully mimic the cellular composition, stem-cell hierarchy and epithelial cell architecture of the *in vivo* intestinal epithelium (Sato et al., 2009), including centrosomal and microtubule reorganization during differentiation (Goldspink et al., 2017a,b). We confirmed Mcc centrosomal localization within the crypt-like domain and at

Journal of Cell Science (2022) 135, jcs259272. doi:10.1242/jcs.259272

Fig. 4. Phosphorylation by CK1δ/ε triggers MCC redeployment to the apical membrane of villus cells. (A) Western blot for MCC in SW480 colon cancer cells. Treatment with PF67046 (5 µM and 10 µM) eliminates phosphorylated MCC (asterisk; the higher molecular mass in the DMSO lane). (B) Co-expression of Myc–MCC and FLAG–CK1ε in HEK293 cells results in the phosphorylation of Myc–MCC (asterisk, lane 2). Phosphorylation of MCC is not observed with CK1ε-D128A (catalytically inactive). (C) Treatment with PF670462 eliminates the phosphorylated form of Myc–MCC (upper band, asterisk) in HEK293 cells co-transfected with FLAG–CK1ε. (D) Co-expression of Myc–MCC and FLAG–CK1ε in HEK293 cells followed by immunoblotting analysis reveals that the interaction of MCC with RASAL2 is stabilized upon MCC phosphorylation, whereas the interaction with NDE1 is weakened. Images are representative of *n*=3. IP, immunoprecipitation; IB, immunoblot; WCL, whole-cell lysates; Ø, empty vector. (E,F) Wholemount bright-field images of mouse wild-type (WT) small-intestinal organoids and (F) WT organoids treated with 5 µM of PF670462. (G) Immunofluorescence (IF) showing Mcc localization along the apical membrane of differentiated cells in WT organoids. (H) IF showing Mcc localization at the apical membrane is disrupted upon treatment with 5 µM of PF670462 in WT organoids. White-dashed squares highlight regions selected for higher magnification. Images are representative of *n*=3. Scale bars: 50 µm. (I,J) Working model for MCC redeployment during intestinal cell differentiation. (I) Phosphorylation of MCC by CK1δ/ε releases MCC from the MTOC by decreasing its affinity to centrosomal proteins such as NDE1. 'X' is an unidentified WNT signal. (J) MCC relocalizes to the ncMTOC, interacting with NHERF1 at the apical membrane and with SCRIB at the apico-lateral junction.

the apical ncMTOC of differentiated cells in the villus-like domain by co-immunostaining for ninein and the membrane marker β-catenin (Fig. S4A,B). Next, organoids were treated with PF670462 on days 3, 4 and 5 post seeding (Fig. 4E,F). Mcc localization was analyzed by IF in sections of PF670462-treated and non-treated control (NTC) organoids. Notably, whereas the Mcc signal was, as expected, detected along the apical membrane facing the central lumen of NTC organoids (Fig. 4G; Fig. S4A–C), Mcc failed to relocalize to the ncMTOC upon inhibition of CK1δ/ε phosphorylation (Fig. 4H; Fig. S4D). To validate these findings, we further evaluated whether the PF670462 treatment affected cellular differentiation and polarization. In PF670462-treated organoids, we observed cell proliferation in crypt domains by Ki67 immunostaining (Fig. S4E,F) and in fully polarized differentiated cells, as demonstrated by alkaline phosphatase staining (Fig. S4G, H) along the apical membrane. These results provide compelling evidence that MCC is a direct target of CK1ε phosphorylation, which decreases the binding of MCC to centrosomal proteins such as NDE1 and triggers the relocalization of MCC to the apical membrane of differentiated intestinal cells (Fig. 4I,J).

DISCUSSION

In this study, we extend our previous findings by comprehensively characterizing *Mcc* transcript expression and Mcc protein localization at the cellular level in the adult mouse SI and colon (Young et al., 2011). Our findings show that *Mcc* is broadly expressed in proliferating cells within intestinal crypts, extending distally from the CBC stem cells at the crypt base into the TA compartment. Notably, no expression of *Mcc* mRNA was observed in SI villus differentiated cells, thus christening *Mcc* as a novel marker for proliferating crypt cells (Fig. 1; Fig. S1). Differences in gene expression patterns along the crypt–villus axis during cell differentiation have been previously described (Velcich et al., 2005). These transcriptional differences reflect the morphological changes that these cells undergo as they progress through differentiation. For example, the MTOC function is reassigned to the apical ncMTOC in villus cells, and this event is accompanied by the transcriptional downregulation of centrosomal genes, redeployment of centrosomal proteins to the apical cell domain, reorganization of microtubules into apicobasal arrays and microvilli assembly (Sen et al., 2010; Ito and Bettencourt-Dias, 2018; Muroyama and Lechler, 2017; Sanchez and Feldman, 2017; Muroyama et al., 2018; Salas, 1999).

Earlier studies using immunohistochemistry and immunoelectron microscopy have described the presence of Mcc at the lateral membrane of murine SI epithelial cells and at the apical cytoplasm of colonic epithelial cells (Senda et al., 1999, 1997; Matsumine et al., 1996). Our IF and confocal microscopy analysis provide incontrovertible evidence that Mcc specifically localizes to the centrosome (MTOC) in crypt cells within the mouse and human intestinal epithelium. In contrast to *Mcc* mRNA distribution, the Mcc protein is additionally found in differentiated cells in the villus, explicitly localizing along the apical membrane – to the ncMTOC. The relocalization of Mcc follows the intracellular trajectory of cardinal centrosomal proteins such as ninein in intestinal cells (Goldspink et al., 2017b; Mogensen et al., 2000), and pericentrin, which colocalizes with Mcc at the centrosome in the crypt and at the ncMTOC in the villus as shown in Fig. 3 and Fig. S3. The shuttling of ninein is proposed to occur via CLIP-170 to ncMTOCs, where it is captured by IQGAP1, an MCC-interacting protein (Fig. 2A) (Goldspink et al., 2017b). To date, however, the molecular mechanisms orchestrating redeployment of centrosomal proteins remain poorly characterized (Muroyama and Lechler, 2017; Sanchez and Feldman, 2017; Paz and Lüders, 2018; Gillard et al., 2021).

MCC is a known phosphoprotein, containing multiple potential serine and tyrosine phosphorylation sites (Pangon et al., 2012; Caria et al., 2019; Arnaud et al., 2009), and our proteomics studies confirm that MCC interacts with the serine/threonine kinases CK1δ/ε in HEK293 cells (Fig. 2A). In agreement, a previous large-scale comparative analysis of the interactomes of 32 human kinases identified MCC as an interactor of CSNK1E (Varjosalo et al., 2013). MCC was also recovered as a prey in another independent affinity purification MS proteomics study in HeLa cells using CSNK1E as a bait (Hein et al., 2015). Given the well-established role of casein kinases as intracellular effectors of the WNT signaling pathway (Gao et al., 2002; Cruciat, 2014; Su et al., 2018), we hypothesized that CK1 activation downstream of an unidentified WNT signal ('X' in Fig. 4I) results in the phosphorylation of Mcc, triggering its relocalization to the ncMTOC during intestinal cellular differentiation. In support of this hypothesis, we first provide evidence that CK1ε phosphorylates MCC (Fig. 4A–C). Second, in small intestinal organoids treated with PF670462, Mcc is no longer found apically in differentiated cells, but is dispersed throughout the cytoplasm (Fig. 4; Fig. S5). A previous study reported that genetic co-depletion of CK1δ and CK1ε significantly impacts the murine intestinal stem cell niche, resulting in epithelial breakdown and rapid death *in vivo* (Morgenstern et al., 2017). These results guided both the low concentration of PF670462 (5 µM) selected and the treatment window of our assay (Fig. 4E–H). The phenotype observed in treated organoids (Fig. 4G) is most likely attributed to the inhibition of Ck1δ/ε activity, which affects overall organoid development, as evidenced by there being fewer Ki67-positive cells in the crypt domain. Consequently, the size of PF670462-treated organoids is relatively smaller than that of non-treated controls. Differentiation and polarity are, however, not affected as demonstrated by IAP staining along the apical membrane of differentiated villus cells (Fig. S4). Future analyses are warranted to investigate the signaling network by which CK1δ/ε activity triggers

Journal of Cell Science (2022) 135, jcs259272. doi:10.1242/jcs.259272

the release–shuttle–capture of centrosomal proteins like MCC to the ncMTOC in differentiated intestinal cells.

Studies are additionally required to better establish the interactome of MCC in intestinal epithelial cells. One limitation of our proteomic experiments is the use of the heterologous aneuploid HEK293 cell line. Although MCC localizes to the centrosome in these cells, it is important to emphasize that these cells are likely of adrenal origin (Lin et al., 2014). Therefore, it is essential to identify endogenous intestinal MCC-binding proteins not recovered in HEK293 cells. One such protein is ezrin, whose interaction with MCC and NHERF1 has been previously reported (Reczek et al., 1997; Morales et al., 2004, 2007; Arnaud et al., 2009; Ewing et al., 2007). NHERF1 is a PDZ scaffold for the ezrin-radixin-moesin (ERM) protein family in epithelial cells (Solinet et al., 2013; Reczek et al., 1997), and ezrin is the only ERM found in the intestinal epithelium (Berryman et al., 1993; Reczek et al., 1997). The binding of ezrin to NHERF1 via PDZ domains in intestinal cells is essential for the assembly of apical protein complexes, their interaction with the cytoskeleton and the establishment of cell polarity (Bretscher et al., 2002; Berryman et al., 1993; Garbett et al., 2010). β-catenin and YAP are known interactors of NHERF1 (Shibata et al., 2003; Mohler et al., 1999). Thus, we postulate that the PBM of MCC interacts with NHERF1–ezrin at the apical membrane of intestinal cells and is potentially involved in establishing cell polarity and intracellular architecture.

Homozygous *Mcc*-null mutant mice have been reported by us and others to be viable and fertile with no ostensible phenotypes (Young et al., 2011; Currey et al., 2019). The interactions of MCC and its cellular localization do, however, invite a more rigorous analysis of the intestinal epithelium in *Mcc*-deficient animals. For example, both *Nherf1*- and ezrin-deficient mice present intestinal phenotypes, including polarity defects and epithelial cellular disorganization (Casaletto et al., 2011; Garbett et al., 2010; Morales et al., 2004; Saotome et al., 2004). Like *Mcc*, homozygous loss of *Nherf1* does not trigger adenoma formation along the length of the intestine (Young et al., 2011; Currey et al., 2019; Georgescu et al., 2016). In a recent study using the sulindac injury model, *Mcc* deficiency was shown to drive inflammation-associated colon cancer (Currey et al., 2019). Moreover, loss of *Nherf1* in combination with $Apc^{Min/+}$ resulted in high levels of cytoplasmic β-catenin and nuclear YAP, and upregulation of the WNT target gene cyclin D1 causing a significant increase in tumor burden (Georgescu et al., 2016). Given the prominent protein–protein interaction between NHERF1 and MCC and the evolutionarily conserved genetic linkage between *APC* and MCC (Luongo et al., 1993), suggesting that these two genes form a synexpression group (Niehrs and Pollet, 1999), it would be interesting to introduce the *Mcc*-null mutation onto the sensitized, cancer-prone Apc^{Min} genetic background (Luongo et al., 1993; Su et al., 1992). As ncMTOC components perform pivotal roles in many cellular processes by regulating and reorganizing microtubules during cell differentiation, we anticipate that the loss of Mcc disrupts protein complexes in differentiated intestinal cells, leading to dysregulation of cell polarity and tissue homeostasis. The generation of mice lacking *Mcc* in the context of Apc^{Min} might reveal subtle, hitherto unappreciated contributions of ncMTOC components and microtubules to intestinal tumor development.

MATERIALS AND METHODS

Human tissues

Paraformaldehyde-fixed paraffin-embedded (PFPE) human intestinal tissue sections were provided by Christopher S. Williams (Vanderbilt University Medical Center, Nashville, TN 37232, USA). Tissues were acquired after informed consent, and clinical investigations were conducted according to the principles expressed in the Declaration of Helsinki and in accordance with the ethical regulations of the Department of Medicine and Cancer Biology at Vanderbilt University School of Medicine, Nashville, TN 37232, USA.

Animals

Mice used for this study were housed, bred and euthanized according to the Institutional Animal Care and Use Committee (IACUC) of Singapore under the protocol number #A20027. This study was performed following all ethical regulations of the Animal Research Facility (ARF) from the Lee Kong Chian School of Medicine (LKCMedicine), Nanyang Technological University (NTU). Experiments were conducted using animals with a minimum age of 90 days. Mcc^{lacZ} mutant mice and wild-type littermates were genotyped as previously described (Young et al., 2011).

Mouse small intestine villi and crypts isolation

Villus and crypt compartments from mouse duodenum were dissociated as previously described (Sato et al., 2009; Goldspink et al., 2017a). Briefly, duodenum (8–10 cm) segments were washed with ice cold 1× PBS-0 (lacking Mg^{2+} and Ca^{2+}). Specimens were cut open longitudinally, and villus fractions were harvested and collected into 50 ml Falcon conical tubes with ice-cold PBS-0. Crypt fractions were filtered through a 70 µm cell strainer (Biosciences #352350). Purified crypt and villus fractions were further processed either for RNA isolation, protein extraction, immunohistochemistry or 3D organoid culture.

Intestinal organoid culture

About 50 isolated crypts/well were seeded in 50 µl of Matrigel (Corning #356231) and cultured in 48-well plates (Corning cat# 3526) using Mouse IntestiCult™ Organoid Growth Medium (Stemcell Technologies #06005) supplemented with 100 mg/ml ampicillin (Sigma #A0166) and 100 mg/ml Primocin (Invivogen #ANTPM1) following the manufacturers' instructions. Only primary cells from mice were used for organoid culture. For inhibition of phosphorylation, fresh culture medium (300 µl) containing 5 µM of the casein kinase 1 δ/ε inhibitor PF670462 (Sigma #SML0795) was changed on days 3, 4 and 5 of culture to consistently maintain a 5 µM concentration of the inhibitor. Treated and non-treated control organoids were harvested on day 6 for histological analysis.

Cell culture

Retinal pigment epithelial (RPE-1, #CRL-4000, ATCC) and human embryonic kidney (HEK293, #85120602, Sigma) cells were cultured in Dulbecco's Modified Eagle Medium (DMEM) high glucose (Gibco #11960-044) supplemented with 10% (v/v) fetal bovine serum (FBS) (Sigma #F2442). Human colon carcinoma HCT116 cells (#91091005, Sigma) were cultured in McCoy's 5A modified medium (Gibco #16600-082) supplemented with 10% (v/v) FBS. Human colon cancer SW480 cells (#CCL-228, ATCC) were cultured in RPMI medium supplemented with 10% (v/v) FBS, 2 mM L-glutamine (Gibco #25030-081), 1 mM sodium pyruvate (Gibco #11360-070) and penicillin-streptomycin (Gibco #15140-122).

Histology

The proximal portion of the small intestine (duodenum) and distal portion of the colon were used for the histological analyses. Tissues were carefully flushed with ice-cold PBS, cut open longitudinally and fixed overnight at 4°C with 4% paraformaldehyde (PFA; EMS #15710). Specimens (roughly 3-cm pieces) were later dehydrated and embedded in paraffin. For whole-mount tissue analysis, samples were fixed overnight with 4% PFA and washed with PBS. Staining for β-galactosidase activity was performed as described in Merkwitz et al. (2016). Alkaline phosphatase staining was performed using the Vulcan Fast Red Chromogen kit (Biocare Medical #FR805S). ISH was performed using RNAscope® 2.5 HD Reagent Kit-Brown (#322300) and 2.5 HD Duplex Reagent Kit (#322430) from Advanced Cell Diagnostics (ACD). The specificity of the Mm*Mcc* probe set (ACD #411961 and #411961-C2) was confirmed by lack of signal in

sections of *Mcc*^{lacZ} homozygous adult intestine. Other probes used were: Mm-*Lgr5* (ACD #312171 and #312171-C2) and Mm-*Ppib* (ACD #313911). For immunofluorescence, tissue sections (7 µm) were deparaffinized and rehydrated. Antigen retrieval was performed with Tris-Borate-EDTA buffer using a pressure cooker (2100 Antigen Retriever #R21005 - Aptum Biologics Ltd). Heat-induced epitope retrieval was conducted at 120°C for a 20 min cycle following the manufacturer's instructions. Sections were then blocked with 5% bovine serum albumin (BSA) (Sigma #A3311) in PBS for 2 h at room temperature (RT) and stained overnight with primary antibodies (Table S1). Primary antibodies were diluted with 1% BSA and 1% goat serum (Sigma G9023) in PBS. Tissues were washed with 0.2% Triton X-100 (Sigma #9002-93-1) in PBS before incubation with secondary antibodies for 1 h at RT. Secondary antibodies were diluted with 1% BSA and 1% Goat Serum (Sigma G9023) in PBS. Each antibody was diluted at the optimal concentration following the manufacturer's instructions. Nuclei were stained with Hoechst 33342 (Thermo Fisher Scientific #62249). Slides were mounted with water-based mounting medium Hydromount (EMS #17966). Representative images of three repeats are included in the manuscript.

Immunofluorescence of cells

RPE-1, HCT116, HEK293 and SW480 cells were grown on glass coverslips and fixed in cold 100% methanol for 20 mins at −20°C. Cells were washed/permeabilized with 0.5% Triton X-100 (Sigma #X100) in PBS and then blocked for 30 min with 5% BSA in 0.1% Triton-X100 in PBS. Immunostaining with primary antibodies (Table S1) was performed overnight at RT followed by PBS washes. Incubation with secondary antibody (Table S1) was performed for 2 h at room temperature. Nuclei were stained using Hoechst 33342 (#62249, Thermo Fisher Scientific). Slides were mounted with water-based mounting medium Hydromount. For SIM, cells were grown on a 1.5H circular glass coverslip, stained and mounted with VECTASHIELD mounting medium (Vector Laboratories #H-1000).

Imaging

Confocal microscopy images were acquired using Olympus FV1000 upright, Olympus FV3000 laser scanning, or Zeiss LSM800 Airyscan microscopes. Objective lenses used for confocal imaging were: (magnification/numerical aperture) 20×/0.75 (air, UPlanSApo), 40×/1.30 (oil, UplanFL N) and 60×/1.35 (oil, UplanSApo). A DeltaVision OMX 3D-SIM Oxford Nanoimager microscope was used for 3D Structured Illumination Microscopy (SIM). SIM images were acquired using 100×/1.40 PSF (oil, UPlanSApo/UIS2) objective lens. Conventional bright-field images were taken using Zeiss AxioImager Z1 upright (ZAZ1). Bright-field images were acquired using the following objective lenses (magnification/numerical aperture): 20×/0.75 NA (air, Plan-Apochromat), 40×/1.3 (oil, ECPlan-Neofluar), 63×/1.4 (oil, Plan-Apochromat), and 100×/1.4 (oil, Plan-Aprochromat). Confocal and bright-field images were further processed using Fiji and 3D SIM video and images were processed with Imaris. The instruments used are either from the A*STAR Microscopy Platform (FV1000, FV3000, ZAZ1 and OMX) or from the LKCMedicine – NTU (LSM800). Confocal images were acquired using the following objective lenses (magnification/numerical aperture): 20×/0.75 (air, UPlanSApo), 40X/1.30 (oil, UplanFL N), and 60×/1.35 (oil, UplanSApo). SIM images were acquired using 100×/1.40 PSF (oil, UPlanSApo / UIS2).

RNA isolation and qPCR

RNA extraction from tissues was performed using TRIzol (Invitrogen #15596026) and an RNeasy kit (Qiagen # 74004). A High-Capacity cDNA Reverse Transcription Kit (Applied Biosystems #4368814) was used for cDNA synthesis. Quantification of gene expression by qPCR was performed using Power SYBR Green PCR Master Mix (Applied Biosystems #4309155). Technical triplicates for a minimum of three biological replicates were used. Relative gene expression was assessed using double CT method and data were normalized to the value for β-actin. Data were tested for significance with an unpaired two-tailed *t*-test. *P*-values of statistical significance are represented as ***P<0.001 and **P<0.01. The qPCR primers are listed in Table S1.

Protein extraction and western blotting

Tissue and cell lysates were prepared using RIPA (Sigma #R0278) lysis buffer supplemented with cOmplete-ULTRA protease inhibitor (Roche #05892970001). Tissue lysates were later sonicated on a Vibra Cell ultrasonic processor (#VCX 130 – SONICS) for two cycles at 4°C for complete lysis. Protein concentration was determined using the Bradford assay. Samples were boiled at 95°C for 5 min. After electrophoresis, proteins were transferred onto a PVDF membrane (Millipore #ISEQ20200) and incubated 1 h at room temperature with 2% milk powder and 0.2% Triton X-100 (Sigma #9002-93-1) in PBS for blocking. Primary antibodies were applied overnight at 4°C in 1% milk powder in PBS at concentrations indicated by the manufacturer. Horseradish peroxidase (HRP) secondary antibodies were diluted (1:10,000) in 1% milk powder in PBS for 1 h at room temperature. Blots were revealed using SuperSignal (Thermo Fisher Scientific #34095). Experiments were performed in triplicates (n=3). β-actin was routinely used as a loading control. Western blot quantification analysis was performed using ImageJ following Hossein Davarinejad's method (York University – Canada; see https://www.yorku.ca/yisheng/Internal/Protocols/ImageJ.pdf).

Constructs

Full-length cDNA constructs of human MCC (P23508-1), NDE1 and RASAL2 were cloned by PCR into pCMV2B (Flag) and pCMV3B (Myc) constructs (Stratagene). Expression constructs for SCRIB, NHERF1 and CK1E, were generated by Gateway Cloning into pcDNA5 FRT-TO (3X FLAG N-terminus or EGFP N-terminus) vectors (Invitrogen). Point mutations and truncations were generated by site-directed mutagenesis using the QuikChange II Site-Directed mutagenesis kit (Agilent #200524) and verified by sequencing. The pCS2+_EmGFP-Mcc (G3UW40) was previously described in Young et al. (2014). This plasmid robustly produces an N-terminal EmGFP-Mcc fusion protein in heterologous cells. HEK293 cells were transfected with a minimum amount of EmGFP-Mcc yielding a mosaic EmGFP-Mcc signal in Fig. 2C.

Immunoprecipitation and mass spectrometry

For immunoprecipitation, cells were lysed in buffer containing 50 mM HEPES (pH 7.5), 150 mM NaCl, 1% Triton X-100, 10% glycerol, and 1 mM EDTA. Lysates, precleared with protein G–Sepharose 4 beads (GE Healthcare #17-0618-0), were incubated with an anti-Flag monoclonal antibody or anti-GFP polyclonal for 1 h, followed by incubation with protein G–Sepharose beads for 1 h. The beads were subsequently washed three times in the lysis buffer. MCC interaction partners were captured using two approaches (gel-free and gel-digest). In both, N-terminal FLAG-tagged human MCC (P23508-1) constructs (pCMV2B vector) were transfected into HEK293 cells and selected with G418 (Gibco #10131035). G418-resistant cells were grown, lysed and immunoprecipitated using anti-FLAG agarose beads. Cells stably expressing an empty vector were used as control. To capture interactions, samples were run either on an SDS-PAGE gel (gel digestion approach) or eluted using 200 mM glycine pH 2.5 (gel-free approach). Samples eluted with glycine were subjected to separation with a strong-cation exchange (SCX) column (Sepax Tech #Z777148) followed by digestion with trypsin (Gibco #R001100). SDS-PAGE gel samples were run against an empty vector control (*pCMV* empty) and bands present in the FLAG–MCC lane were extracted and digested. Samples were subjected to liquid chromatography and mass spectrometry (on an Orbitrap classic or an Orbitrap Velos). Raw files were converted to mzML and mzXML files and searched using Comet, version 2012.02rev.0 (Eng et al., 2013) against the NCBI RefSeq database (version 57, January 30, 2013) containing a total of 72,482 human and adenovirus sequences supplemented with common contaminants from the Max Planck Institute and the Global Proteome Machine (GPM; https://www.thegpm.org/crap/index.html). The database parameters were set to search for tryptic cleavages, permitting up to two missed cleavage sites per peptide with a mass tolerance of 10 or 12 ppm for precursors with charges +2 to +4 and a tolerance of ±0.5 amu for fragment ions. Cysteine carbamidomethyl was used as a fixed modification and

methionine oxidation was allowed as a variable modification. The results from each search engine were subsequently analyzed through the Trans-Proteomic Pipeline (version 4.6 Occupy rev 3) using the iProphet pipeline (Shteynberg et al., 2011) implemented within ProHits (Liu et al., 2016). Data were transferred to the Analyst module of ProHits, and proteins identified with ≥2 unique peptides and an iProphet probability ≥0.95 were analyzed through Significance Analysis of INTeractome (SAINTexpress, version 3.6.1; Teo et al., 2014). SAINTexpress analysis was performed using the default parameters by comparing the triplicates of the FLAG–MCC purifications to those of the empty vector controls, and only those entries passing a calculated Bayesian false discovery rate (BFDR) of ≤1% were considered high-confidence interactors. Gene Ontology enrichment evaluation was through g:Profiler, using default options (Raudvere et al., 2019). Data were visualized through ProHits-viz using the Single Condition Visualization tool (Knight et al., 2017). The mass spectrometry data, alongside the annotation and identification files were deposited in the ProteomeXchange server MassIVE (https://massive.ucsd.edu/), as a complete submission and assigned the accession numbers MassIVE ID: MSV000089258 and ProteomeXchange: PXD033261.

Acknowledgements
We thank Drs Radoslaw Sobota (IMCB, Singapore) and Bernett Lee (SIgN, Singapore) for their invaluable assistance with bioinformatics analyses, Drs Brian Burke and Lee Yin Loon (SRIS, Singapore) for insightful discussions about centrosome biology, Dr Graham Wright (A*STAR Microscopy Platform) for technical assistance with SIM, Drs Nicholas Barker (IMCB, Singapore) and Kazuhiro Murakami (Kanazawa University, Japan) for both their helpful discussions and reagents supporting intestinal organoid culture and analysis, and Dr Brigid Hogan for comments on the manuscript. Finally, we wish to honor the legacy and significant scientific contributions of the late Professor Tony Pawson (2013) in whose lab B.A.L. first discovered the centrosomal localization of MCC.

Competing interests
The authors declare no competing or financial interests.

Author contributions
Conceptualization: L.B.T., B.A.L., N.S.T., N.R.D.; Methodology: L.B.T., B.A.L., N.S.T., N.R.D.; Software: L.B.T., B.A.L., A.G., N.R.D.; Validation: L.B.T., B.A.L., N.R.D.; Formal analysis: L.B.T., B.A.L., M.M., S.L.O., E.K.T., N.S.T., C.S.W., A.G., M.L., N.R.D.; Investigation: L.B.T., B.A.L., N.S.T., M.L., N.R.D.; Resources: C.S.W., A.G., N.R.D.; Data curation: L.B.T., B.A.L., M.L., N.R.D.; Writing - original draft: L.B.T., M.L., N.R.D.; Writing - review & editing: L.B.T., N.R.D.; Visualization: L.B.T., N.R.D.; Supervision: N.R.D.; Project administration: L.B.T., N.R.D.; Funding acquisition: N.R.D.

Funding
This work was funded by the Institute of Medical Biology [Agency for Science, Technology and Research (A*STAR), Singapore] as well as start-up funding provided by the Lee Kong Chian School of Medicine, Nanyang Technological University and the Ministry of Education (MOE), Singapore [Continuation Grant – Endodermal Development and Differentiation (EDD) Lab] to N.R.D. L.B.T. was initially funded by the Singapore International Graduate Award (SINGA), A*STAR Graduate Academy (A*GA). B.A.L. was funded by a Canadian Institute of Health Research postdoctoral fellowship.

Data availability
The mass spectrometry data, alongside the annotation and identification files were deposited in the ProteomeXchange server MassIVE (massive.ucsd.edu), as a complete submission and assigned the accession numbers MassIVE ID: MSV000089258 and ProteomeXchange: PXD033261.

Peer review history
The peer review history is available online at https://journals.biologists.com/jcs/lookup/doi/10.1242/jcs.259272.reviewer-comments.pdf.

References
Arnaud, C., Sebbagh, M., Nola, S., Audebert, S., Bidaut, G., Hermant, A., Gayet, O., Dusetti, N. J., Ollendorff, V., Santoni, M.-J. et al. (2009). MCC, a new interacting protein for Scrib, is required for cell migration in epithelial cells. *FEBS Lett.* **583**, 2326-2332. doi:10.1016/j.febslet.2009.06.034

Ashton-Rickardt, P. G., Wyllie, A. H., Bird, C. C., Dunlop, M. G., Steel, C. M., Morris, R. G., Piris, J., Romanowski, P., Wood, R. and White, R. (1991). MCC, a candidate familial polyposis gene in 5q.21, shows frequent allele loss in colorectal and lung cancer. *Oncogene* **6**, 1881-1886.

Badura, L., Swanson, T., Adamowicz, W., Adams, J., Cianfrogna, J., Fisher, K., Holland, J., Kleiman, R., Nelson, F., Reynolds, L. et al. (2007). An inhibitor of casein kinase Iε induces phase delays in circadian rhythms under free-running and entrained conditions. *J. Pharmacol. Exp. Ther.* **322**, 730-738. doi:10.1124/jpet.107.122846

Barker, N. (2014). Adult intestinal stem cells: critical drivers of epithelial homeostasis and regeneration. *Nat. Rev. Mol. Cell Biol.* **15**, 19-33. doi:10.1038/nrm3721

Barker, N., van Es, J. H., Kuipers, J., Kujala, P., van den Born, M., Cozijnsen, M., Haegebarth, A., Korving, J., Begthel, H., Peters, P. J. et al. (2007). Identification of stem cells in small intestine and colon by marker gene Lgr5. *Nature* **449**, 1003-1007. doi:10.1038/nature06196

Benthani, F. A., Herrmann, D., Tran, P. N., Pangon, L., Lucas, M. C., Allam, A. H., Currey, N., Al-Sohaily, S., Giry-Laterriere, M., Warusavitarne, J. et al. (2018). 'MCC' protein interacts with E-cadherin and β-catenin strengthening cell–cell adhesion of HCT116 colon cancer cells. *Oncogene* **37**, 663-672. doi:10.1038/onc.2017.362

Berryman, M., Franck, Z. and Bretscher, A. (1993). Ezrin is concentrated in the apical microvilli of a wide variety of epithelial cells whereas moesin is found primarily in endothelial cells. *J. Cell Sci.* **105**, 1025-1043. doi:10.1242/jcs.105.4.1025

Bouckson-Castaing, V., Moudjou, M., Ferguson, D. J., Mucklow, S., Belkaid, Y., Milon, G. and Crocker, P. R. (1996). Molecular characterisation of ninein, a new coiled-coil protein of the centrosome. *J. Cell Sci.* **109**, 179-190. doi:10.1242/jcs.109.1.179

Bourne, H. R. (1991). Consider the coiled coil. *Nature* **351**, 188-189. doi:10.1038/351188a0

Bretscher, A., Edwards, K. and Fehon, R. G. (2002). ERM proteins and merlin: integrators at the cell cortex. *Nat. Rev. Mol. Cell Biol.* **3**, 586-599. doi:10.1038/nrm882

Brinkley, B. R. (1985). Microtubule organizing centers. *Annu. Rev. Cell Dev. Biol.* **1**, 145-172. doi:10.1146/annurev.cb.01.110185.001045

Caria, S., Stewart, B. Z., Jin, R., Smith, B. J., Humbert, P. O. and Kvansakul, M. (2019). Structural analysis of phosphorylation–associated interactions of human MCC with Scribble PDZ domains. *FEBS J.* **286**, 4910-4925. doi:10.1111/febs.15002

Casaletto, J. B., Saotome, I., Curto, M. and McClatchey, A. I. (2011). Ezrin-mediated apical integrity is required for intestinal homeostasis. *Proc. Natl. Acad. Sci. USA* **108**, 11924-11929. doi:10.1073/pnas.1103418108

Clevers, H. (2013). The intestinal crypt, a prototype stem cell compartment. *Cell* **154**, 274-284. doi:10.1016/j.cell.2013.07.004

Cruciat, C.-M. (2014). Casein kinase 1 and Wnt/β-catenin signaling. *Curr. Opin. Cell Biol.* **31**, 46-55. doi:10.1016/j.ceb.2014.08.003

Currey, N., Jahan, Z., Caldon, C. E., Tran, P. N., Benthani, F., Lacavalerie, P. D., Roden, D. L., Gloss, B. S., Campos, C., Bean, E. G. et al. (2019). Mouse model of "Mutated in Colorectal Cancer" gene deletion reveals novel pathways in inflammation and cancer. *Cell Mol. Gastroenterol. Hepatol.* **7**, 819-839. doi:10.1016/j.jcmgh.2019.01.009

Doxsey, S. J., Stein, P., Evans, L., Calarco, P. D. and Kirschner, M. (1994). Pericentrin, a highly conserved centrosome protein involved in microtubule organization. *Cell* **76**, 639-650. doi:10.1016/0092-8674(94)90504-5

Eng, J. K., Jahan, T. A. and Hoopmann, M. R. (2013). Comet: an open-source MS/MS sequence database search tool. *Proteomics* **13**, 22-24. doi:10.1002/pmic.201200439

Ewing, R. M., Chu, P., Elisma, F., Li, H., Taylor, P., Climie, S., McBroom–Cerajewski, L., Robinson, M. D., O'Connor, L., Li, M. et al. (2007). Large–scale mapping of human protein–protein interactions by mass spectrometry. *Mol. Syst. Biol.* **3**, 89. doi:10.1038/msb4100134

Fukuyama, R., Niculaita, R., Ng, K. P., Obusez, E., Sanchez, J., Kalady, M., Aung, P. P., Casey, G. and Sizemore, N. (2008). Mutated in colorectal cancer, a putative tumor suppressor for serrated colorectal cancer, selectively represses β-catenin-dependent transcription. *Oncogene* **27**, 6044-6055. doi:10.1038/onc.2008.204

Gao, Z.-H., Seeling, J. M., Hill, V., Yochum, A. and Virshup, D. M. (2002). Casein kinase I phosphorylates and destabilizes the β-catenin degradation complex. *Proc. Natl. Acad. Sci. USA* **99**, 1182-1187. doi:10.1073/pnas.032468199

Garbett, D., LaLonde, D. P. and Bretscher, A. (2010). The scaffolding protein EBP50 regulates microvillar assembly in a phosphorylation-dependent manner. *J. Cell Biol.* **191**, 397-413. doi:10.1083/jcb.201004115

Gehart, H. and Clevers, H. (2019). Tales from the crypt: new insights into intestinal stem cells. *Nat. Rev. Gastroenterol. Hepatol.* **16**, 19-34. doi:10.1038/s41575-018-0081-y

Georgescu, M.-M., Gagea, M. and Cote, G. (2016). NHERF1/EBP50 suppresses Wnt-β-catenin pathway–driven intestinal neoplasia. *Neoplasia* **18**, 512-523. doi:10.1016/j.neo.2016.07.003

Gillard, G., Girdler, G. and Röper, K. (2021). A release-and-capture mechanism generates an essential non-centrosomal microtubule array during tube budding. *Nat. Commun.* **12**, 4096. doi:10.1038/s41467-021-24332-0

Goldspink, D. A., Matthews, Z. J., Lund, E. K., Wileman, T. and Mogensen, M. M. (2017a). Immuno-fluorescent labeling of microtubules and centrosomal proteins in ex vivo intestinal tissue and 3D in vitro intestinal organoids. *J. Vis. Exp.* **130**, 56662. doi:10.3791/56662

Goldspink, D. A., Rookyard, C., Tyrrell, B. J., Gadsby, J., Perkins, J., Lund, E. K., Galjart, N., Thomas, P., Wileman, T. and Mogensen, M. M. (2017b). Ninein is essential for apico-basal microtubule formation and CLIP-170 facilitates its redeployment to non-centrosomal microtubule organizing centres. *Open Biol.* **7**, 160274. doi:10.1098/rsob.160274

Greer, Y. E., Westlake, C. J., Gao, B., Bharti, K., Shiba, Y., Xavier, C. P., Pazour, G. J., Yang, Y. and Rubin, J. S. (2014). Casein kinase 1δ functions at the centrosome and Golgi to promote ciliogenesis. *Mol. Biol. Cell* **25**, 1629-1640. doi:10.1091/mbc.e13-10-0598

Groden, J., Thliveris, A., Samowitz, W., Carlson, M., Gelbert, L., Albertsen, H., Joslyn, G., Stevens, J., Spirio, L., Robertson, M. et al. (1991). Identification and characterization of the familial adenomatous polyposis coli gene. *Cell* **66**, 589-600. doi:10.1016/0092-8674(81)90021-0

Hein, M. Y., Hubner, N. C., Poser, I., Cox, J., Nagaraj, N., Toyoda, Y., Gak, I. A., Weisswange, I., Mansfeld, J., Buchholz, F. et al. (2015). A human interactome in three quantitative dimensions organized by stoichiometries and abundances. *Cell* **163**, 712-723. doi:10.1016/j.cell.2015.09.053

Heintzmann, R. and Huser, T. (2017). Super-resolution structured illumination microscopy. *Chem. Rev.* **117**, 13890-13908. doi:10.1021/acs.chemrev.7b00218

Hinnebusch, B. F., Siddique, A., Henderson, J. W., Malo, M. S., Zhang, W., Athaide, C. P., Abedrapo, M. A., Chen, X., Yang, V. W. and Hodin, R. A. (2004). Enterocyte differentiation marker intestinal alkaline phosphatase is a target gene of the gut-enriched Krüppel-like factor. *Am. J. Physiol. Gastrointest. Liver Physiol.* **286**, G23-G30. doi:10.1152/ajplung.00352.2002

Hua, K. and Ferland, R. J. (2017). Fixation methods can differentially affect ciliary protein immunolabeling. *Cilia* **6**, 5. doi:10.1186/s13630-017-0045-9

Ito, D. and Bettencourt-Dias, M. (2018). Centrosome remodelling in evolution. *Cells* **7**, 71. doi:10.3390/cells7070071

Keenan, C. R., Langenbach, S. Y., Jativa, F., Harris, T., Li, M., Chen, Q., Xia, Y., Gao, B., Schuliga, M. J., Jaffar, J. et al. (2018). Casein kinase 1δ/ε inhibitor, PF670462 attenuates the fibrogenic effects of transforming growth factor-β in pulmonary fibrosis. *Front. Pharmacol.* **9**, 738. doi:10.3389/fphar.2018.00738

Kinzler, K., Nilbert, M., Su, L., Vogelstein, B., Bryan, T., Levy, D., Smith, K., Preisinger, A., Hedge, P., McKechnie, D. et al. (1991a). Identification of FAP locus genes from chromosome 5q21. *Science* **253**, 661-665. doi:10.1126/science.1651562

Kinzler, K., Nilbert, M., Vogelstein, B., Bryan, T., Levy, D., Smith, K., Preisinger, A., Hamilton, A. C., Hedge, P., Markham, A. et al. (1991b). Identification of a gene located at chromosome 5q21 that is mutated in colorectal cancers. *Science* **251**, 1366-1370. doi:10.1126/science.1848370

Knight, J. D. R., Choi, H., Gupta, G. D., Pelletier, L., Raught, B., Nesvizhskii, A. I. and Gingras, A.-C. (2017). ProHits-viz: a suite of web tools for visualizing interaction proteomics data. *Nat. Methods* **14**, 645-646. doi:10.1038/nmeth.4330

Leushacke, M. and Barker, N. (2014). Ex vivo culture of the intestinal epithelium: strategies and applications. *Gut* **63**, 1345. doi:10.1136/gutjnl-2014-307204

Lin, Y.-C., Boone, M., Meuris, L., Lemmens, I., Roy, N. V., Soete, A., Reumers, J., Moisse, M., Plaisance, S., Drmanac, R. et al. (2014). Genome dynamics of the human embryonic kidney 293 lineage in response to cell biology manipulations. *Nat. Commun.* **5**, 4767. doi:10.1038/ncomms5767

Liu, G., Knight, J. D. R., Zhang, J. P., Tsou, C.-C., Wang, J., Lambert, J.-P., Larsen, B., Tyers, M., Raught, B., Bandeira, N. et al. (2016). Data Independent Acquisition analysis in ProHits 4.0. *J. Proteomics* **149**, 64-68. doi:10.1016/j.jprot.2016.04.042

Luongo, C., Gould, K. A., Su, L.-K., Kinzler, K. W., Vogelstein, B., Dietrich, W., Lander, E. S. and Moser, A. R. (1993). Mapping of multiple intestinal Neoplasia (Min) to proximal chromosome 18 of the mouse. *Genomics* **15**, 3-8. doi:10.1006/geno.1993.1002

Matsumine, A., Senda, T., Baeg, G.-H., Roy, B. C., Nakamura, Y., Noda, M., Toyoshima, K. and Akiyama, T. (1996). MCC, a cytoplasmic protein that blocks cell cycle progression from the G/G to S phase. *J. Biol. Chem.* **271**, 10341-10346. doi:10.1074/jbc.271.17.10341

Meads, T. and Schroer, T. A. (1995). Polarity and nucleation of microtubules in polarized epithelial cells. *Cell Motil. Cytoskel.* **32**, 273-288. doi:10.1002/cm.970320404

Merkwitz, C., Blaschuk, O., Schulz, A. and Ricken, A. M. (2016). Comments on methods to suppress endogenous β-galactosidase activity in mouse tissues expressing the LacZ reporter gene. *J. Histochem. Cytochem.* **64**, 579-586. doi:10.1369/0022155416665337

Mogensen, M. M., Malik, A., Piel, M., Bouckson-Castaing, V. and Bornens, M. (2000). Microtubule minus-end anchorage at centrosomal and non-centrosomal sites: the role of ninein. *J. Cell Sci.* **113**, 3013-3023. doi:10.1242/jcs.113.17.3013

Mohler, P. J., Kreda, S. M., Boucher, R. C., Sudol, M., Stutts, M. J. and Milgram, S. L. (1999). Yes-associated protein 65 localizes P62c-yes to the apical compartment of airway epithelia by association with Ebp50. *J. Cell Biol.* **147**, 879-890. doi:10.1083/jcb.147.4.879

Morales, F. C., Takahashi, Y., Kreimann, E. L. and Georgescu, M.-M. (2004). Ezrin-radixin-moesin (ERM)-binding phosphoprotein 50 organizes ERM proteins at the apical membrane of polarized epithelia. *Proc. Natl. Acad. Sci. USA* **101**, 17705-17710. doi:10.1073/pnas.0407974101

Morales, F. C., Takahashi, Y., Momin, S., Adams, H., Chen, X. and Georgescu, M.-M. (2007). NHERF1/EBP50 Head-to-Tail Intramolecular Interaction Masks Association with PDZ Domain Ligands. *Mol. Cell. Biol.* **27**, 2527-2537. doi:10.1128/MCB.01372-06

Morgenstern, Y., Adhikari, U. D., Ayyash, M., Elyada, E., Tóth, B., Moor, A., Itzkovitz, S. and Ben–Neriah, Y. (2017). Casein kinase 1–epsilon or 1–delta required for Wnt–mediated intestinal stem cell maintenance. *EMBO J.* **36**, 3046-3061. doi:10.15252/embj.201696253

Muroyama, A. and Lechler, T. (2017). Microtubule organization, dynamics and functions in differentiated cells. *Development* **144**, 3012-3021. doi:10.1242/dev.153171

Muroyama, A., Terwilliger, M., Dong, B., Suh, H. and Lechler, T. (2018). Genetically induced microtubule disruption in the mouse intestine impairs intracellular organization and transport. *Mol. Biol. Cell* **29**, 1533-1541. doi:10.1091/mbc.E18-01-0057

Niehrs, C. and Pollet, N. (1999). Synexpression groups in eukaryotes. *Nature* **402**, 483-487. doi:10.1038/990025

Nishisho, I., Nakamura, Y., Miyoshi, Y., Miki, Y., Ando, H., Horii, A., Koyama, K., Utsunomiya, J., Baba, S. and Hedge, P. (1991). Mutations of chromosome 5q21 genes in FAP and colorectal cancer patients. *Science* **253**, 665-669. doi:10.1126/science.1651563

Oughtred, R., Rust, J., Chang, C., Breitkreutz, B., Stark, C., Willems, A., Boucher, L., Leung, G., Kolas, N., Zhang, F. et al. (2021). The BioGRID database: a comprehensive biomedical resource of curated protein, genetic, and chemical interactions. *Protein Sci.* **30**, 187-200. doi:10.1002/pro.3978

Pangon, L., Sigglekow, N. D., Larance, M., Al-Sohaily, S., Mladenova, D. N., Selinger, C. I., Musgrove, E. A. and Kohonen-Corish, M. R. J. (2010). The "mutated in colorectal cancer" protein is a novel target of the UV-induced DNA damage checkpoint. *Genes Cancer* **1**, 917-926. doi:10.1177/1947601910388937

Pangon, L., Kralingen, C. V., Abas, M., Daly, R. J., Musgrove, E. A. and Kohonen-Corish, M. R. J. (2012). The PDZ-binding motif of MCC is phosphorylated at position −1 and controls lamellipodia formation in colon epithelial cells. *Biochim. Biophys. Acta Mol. Cell Res.* **1823**, 1058-1067. doi:10.1016/j.bbamcr.2012.03.011

Pangon, L., Mladenova, D., Watkins, L., Kralingen, C., Currey, N., Al-Sohaily, S., Lecine, P., Borg, J. and Kohonen-Corish, M. R. J. (2015). MCC inhibits beta-catenin transcriptional activity by sequestering DBC1 in the cytoplasm. *Int. J. Cancer* **136**, 55-64. doi:10.1002/ijc.28967

Paz, J. and Lüders, J. (2018). Microtubule-organizing centers: towards a minimal parts list. *Trends Cell Biol.* **28**, 176-187. doi:10.1016/j.tcb.2017.10.005

Peters, J. M., McKay, R. M., McKay, J. P. and Graff, J. M. (1999). Casein kinase I transduces Wnt signals. *Nature* **401**, 345-350. doi:10.1038/43830

Raudvere, U., Kolberg, L., Kuzmin, I., Arak, T., Adler, P., Peterson, H. and Vilo, J. (2019). g:Profiler: a web server for functional enrichment analysis and conversions of gene lists (2019 update). *Nucleic Acids Res.* **47**, W191-W198. doi:10.1093/nar/gkz369

Reczek, D., Berryman, M. and Bretscher, A. (1997). Identification of EBP50: A PDZ-containing phosphoprotein that associates with members of the Ezrin-Radixin-Moesin Family. *J. Cell Biol.* **139**, 169-179. doi:10.1083/jcb.139.1.169

Sakanaka, C., Leong, P., Xu, L., Harrison, S. D. and Williams, L. T. (1999). Casein kinase Iε in the Wnt pathway: regulation of β-catenin function. *Proc. Natl. Acad. Sci. USA* **96**, 12548-12552. doi:10.1073/pnas.96.22.12548

Salas, P. J. I. (1999). Insoluble γ-tubulin–containing structures are anchored to the apical network of intermediate filaments in polarized Caco-2 epithelial cells. *J. Cell Biol.* **146**, 645-658. doi:10.1083/jcb.146.3.645

Sanchez, A. D. and Feldman, J. L. (2017). Microtubule-organizing centers: from the centrosome to non-centrosomal sites. *Curr. Opin. Cell Biol.* **44**, 93-101. doi:10.1016/j.ceb.2016.09.003

Saotome, I., Curto, M. and McClatchey, A. I. (2004). Ezrin is essential for epithelial organization and villus morphogenesis in the developing intestine. *Dev. Cell* **6**, 855-864. doi:10.1016/j.devcel.2004.05.007

Sato, T., Vries, R. G., Snippert, H. J., van de Wetering, M., Barker, N., Stange, D. E., van Es, J. H., Abo, A., Kujala, P., Peters, P. J. et al. (2009). Single Lgr5 stem cells build crypt-villus structures in vitro without a mesenchymal niche. *Nature* **459**, 262-265. doi:10.1038/nature07935

Sen, G. L., Reuter, J. A., Webster, D. E., Zhu, L. and Khavari, P. A. (2010). DNMT1 maintains progenitor function in self-renewing somatic tissue. *Nature* **463**, 563-567. doi:10.1038/nature08683

Senda, T., Matsumine, A., Akiyama, T. and Kobayashi, S. (1997). Association of the MCC gene product with the plasma membrane and membrane organelles. *Med. Electron. Microsc.* **30**, 1-7. doi:10.1007/BF01458345

Senda, T., Matsumine, A., Yanai, H. and Akiyama, T. (1999). Localization of MCC (mutated in colorectal cancer) in various tissues of mice and its involvement in cell differentiation. *J. Histochem. Cytochem.* **47**, 1149-1157. doi:10.1177/002215549904700907

Shibata, T., Chuma, M., Kokubu, A., Sakamoto, M. and Hirohashi, S. (2003). EBP50, a β-catenin-associating protein, enhances Wnt signaling and is over-expressed in hepatocellular carcinoma. *Hepatology* **38**, 178-186. doi:10.1053/jhep.2003.50270

Shteynberg, D., Deutsch, E. W., Lam, H., Eng, J. K., Sun, Z., Tasman, N., Mendoza, L., Moritz, R. L., Aebersold, R. and Nesvizhskii, A. I. (2011). iProphet: multi-level integrative analysis of shotgun proteomic data improves peptide and protein identification rates and error estimates*. *Mol. Cell. Proteomics* **10**, M111.007690. doi:10.1074/mcp.M111.007690

Solinet, S., Mahmud, K., Stewman, S. F., Kadhi, K. B. E., Decelle, B., Talje, L., Ma, A., Kwok, B. H. and Carreno, S. (2013). The actin-binding ERM protein Moesin binds to and stabilizes microtubules at the cell cortex. *J. Cell Biol.* **202**, 251-260. doi:10.1083/jcb.201304052

Su, L.-K., Kinzler, K., Vogelstein, B., Preisinger, A., Moser, A., Luongo, C., Gould, K. and Dove, W. (1992). Multiple intestinal neoplasia caused by a mutation in the murine homolog of the APC gene. *Science* **256**, 668-670. doi:10.1126/science.1350108

Su, Z., Song, J., Wang, Z., Zhou, L., Xia, Y., Yu, S., Sun, Q., Liu, S.-S., Zhao, L., Li, S. et al. (2018). Tumor promoter TPA activates Wnt/β-catenin signaling in a casein kinase 1-dependent manner. *Proc. Natl. Acad. Sci. USA* **115**, E7522-E7531. doi:10.1073/pnas.1802422115

Sussman, N. L., Eliakim, R., Rubin, D., Perlmutter, D. H., DeSchryver-Kecskemeti, K. and Alpers, D. H. (1989). Intestinal alkaline phosphatase is secreted bidirectionally from villous enterocytes. *Am. J. Physiol.* **257**, G14-G23. doi:10.1152/ajpgi.1989.257.1.G14

Teo, G., Liu, G., Zhang, J., Nesvizhskii, A. I., Gingras, A.-C. and Choi, H. (2014). SAINTexpress: improvements and additional features in significance analysis of INTeractome software. *J. Proteomics* **100**, 37-43. doi:10.1016/j.jprot.2013.10.023

Varjosalo, M., Sacco, R., Stukalov, A., van Drogen, A., Planyavsky, M., Hauri, S., Aebersold, R., Bennett, K. L., Colinge, J., Gstaiger, M. et al. (2013). Interlaboratory reproducibility of large-scale human protein-complex analysis by standardized AP-MS. *Nat. Methods* **10**, 307-314. doi:10.1038/nmeth.2400

Velcich, A., Corner, G., Paul, D., Zhuang, M., Mariadason, J. M., Laboisse, C. and Augenlicht, L. (2005). Quantitative rather than qualitative differences in gene expression predominate in intestinal cell maturation along distinct cell lineages. *Exp. Cell Res.* **304**, 28-39. doi:10.1016/j.yexcr.2004.10.014

Waller, A., Findeis, S. and Lee, M. (2016). Familial adenomatous polyposis. *J. Pediatr. Genet.* **05**, 078-083. doi:10.1055/s-0036-1579760

Young, T., Poobalan, Y., Ali, Y., Tein, W. S., Sadasivam, A., Ee Kim, T., Erica Tay, P. E. and Dunn, N. R. (2011). Mutated in colorectal cancer (Mcc), a candidate tumor suppressor, is dynamically expressed during mouse embryogenesis. *Dev. Dyn.* **240**, 2166-2174. doi:10.1002/dvdy.22712

Young, T., Poobalan, Y., Tan, E. K., Tao, S., Ong, S., Wehner, P., Schwenty-Lara, J, Lim, C. Y., Sadasivam, A., Lovatt, M. et al. (2014). The PDZ domain protein Mcc is a novel effector of non-canonical Wnt signaling during convergence and extension in zebrafish. *Development* **141**, 3505-3516. doi:10.1242/dev.114033